AirNet: Energy-Aware Deployment and Scheduling of Aerial Networks

Elif Bozkaya, Klaus-Tycho Foerster, Stefan Schmid, and Berk Canberk *Senior Member, IEEE*

***Abstract*—Aerial Base Stations (ABSs) promise resilient and perpetual connectivity after unexpected events such as natural disasters. However, the deployment and scheduling of ABSs introduce several algorithmic challenges. In particular, on-demand communication can change over time and be hard to accurately predict, so it needs to be handled in an online manner, accounting also for battery consumption constraints. This paper presents *AirNet*, an efficient software-based solution to operate ABSs which meet these requirements. *AirNet* is based on an efficient placement algorithm for ABSs which maximizes the number of covered users, and a scheduler which navigates and recharges ABSs in an energy-aware manner. To this end, we propose an energy-aware deployment algorithm and use an energy model to analyze the power consumption and thereby, improve the flight endurance. In addition, we evaluate a novel scheduling mechanism that efficiently manages the ABSs' operations. Our simulations indicate that our approach can significantly improve the flight endurance and user coverage compared to a recent state-of-the-art approach.**

***Index Terms*—Aerial Base Stations, energy efficiency, endurance, hover time, demand-aware deployment**

I. Introduction

ACCORDING to the Weather, Climate & Catastrophe Insight 2017 Annual Report [1], the direct economic damage of the weather and climate topped USD 353 billion in 2017. Thus, over the last years, interesting novel technologies have emerged for disaster assistance with the highly mobile and low-cost aerial platforms. The aim of such aerial platforms is to meet urgent communication needs in mission critical environments. Especially, the use of Aerial Base Stations (ABSs), e.g. drones, has become a prominent solution: when the existing terrestrial network is temporarily damaged, ABS-based wireless communications can provide adaptive coverage and high service quality for User Equipments (UEs). In addition, it is expected that nearly 12% of global mobile traffic will be 5G cellular connectivity by 2022, where an average 5G connection will generate 21GB traffic per month [2]. Thus, the use of ABSs also assists to increase the coverage of the existing terrestrial networks.

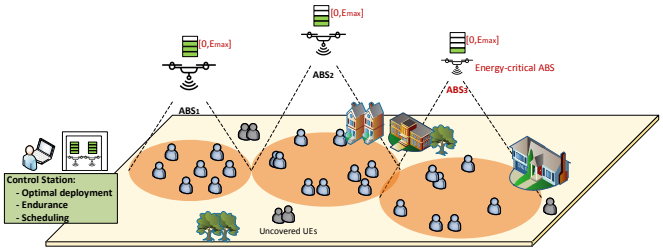

Fig. 1. Considered scenario for aerial networks.

ABS connectivity is built on top of the existing terrestrial wireless networks. Compared to conventional Base Stations (BS), ABSs can adjust their positions and provide on-demand communications to the UEs. However, due to the weight and size constraints, ABSs have limited operational time before the batteries are recharged. Their limited battery capacities affect the network lifetime sacrificing throughput. Although multiple ABSs ensure high service quality to the UEs, they introduce several algorithmic challenges, specifically in terms of energy-aware optimal deployment, flight endurance and scheduling the ABSs' operations. The success of this technology rests on (i) energy efficient deployment and (ii) controlling ABSs' operations in a coordinated manner. Defining ABS positions is an important first step in network planning for long-lived aerial networks. Then, energy saving mechanisms and intelligent duty cycle can be managed by a control station.

In this paper, we focus on a practical scenario, where ABSs provide emergency coverage to the disaster area after failures of the terrestrial BSs as shown in Fig. 1. We provide a coverage model that aims to maximize the hover time through an energy efficient deployment and reduces battery charging time. The control station implements *optimal ABS deployment, maximizing endurance and scheduling for recharging* functionalities to manage ABSs. The control station identifies the optimal subset of UEs, via a deployment algorithm, to assign ABSs. After the placement of ABSs, the control station now tracks the consumed energy to specify the time for which ABSs should be recharged. Thus, the key challenges in creating such a model are: (i) ensuring a coverage model for ABSs from an online perspective, (ii) maximizing the flight endurance to serve UEs as long as possible and (iii) scheduling the operations of ABSs. Note that user demands can vary over time in unpredictable ways and satisfying these demands requires flexibility to reconfigure the network in an

Manuscript received June 4, 2020; revised March 1, 2020; accepted August 21, 2020. Date of publication XXXXXX XX, XXXX; date of current version XXXXXXX XX, XXXX. Elif Bozkaya was supported by The Scientific and Technical Research Council of Turkey (TUBITAK) 2214 International Research Fellowship Programme (for PhD Students). The paper is supported by The Scientific and Technical Research Council of Turkey (TUBITAK) 1001 The Scientific and Technological Research Projects Funding Program with project number 119E434. *(Corresponding author: Elif Bozkaya.)*

E. Bozkaya is with the Department of Computer Engineering, National Defense University Naval Academy and Istanbul Technical University, Istanbul, Turkey and she was also with the Faculty of Computer Science, University of Vienna, Austria e-mail: (bozkayae@itu.edu.tr).

K. T. Foerster and S. Schmid are with the Faculty of Computer Science, University of Vienna, Austria e-mail: (klaus-tycho.foerster@univie.ac.at; stefan_schmid@univie.ac.at).

B. Canberk is with the Department of Computer Engineering, Istanbul Technical University, Istanbul, Turkey e-mail: (canberk@itu.edu.tr).

online manner. Thus, this paper explores a scenario where user demands are not entirely predictable and not known a priori.

More specifically, this paper presents *AirNet*, an energy efficient software-based solution for ABSs that improves user coverage and flight endurance. More specifically, we make the following contributions:

- An energy-optimal placement algorithm is proposed to maximize the number of covered UEs under limited battery capacity and limited number of ABSs. The demand-aware configuration is also analyzed from an online perspective.
- We use an energy model to improve the flight endurance and derive an efficient recharging strategy such that the total energy consumption of all ABSs is minimized. We also consider the affecting parameters including weight, flying time and flying speed.
- A scheduling mechanism is provided to assign ABSs to the limited number of replenishment stations, which can avoid the ABSs from being out of service for a long time.
- We report on an extensive evaluation showing average 24% improvement in the user coverage and 8% extension in the flight endurance compared to a recent state-of-the-art approach [3].

The rest of the paper is organized as follows: We review the related work in Section II. In Section III, we discuss the network architecture and model. In Section IV, we give the *AirNet* system. In Section V, we validate our model with extensive simulations and conclude the paper in Section VI.

II. Related Work

In this section, we will review the related works on energy-efficient deployments and the maximization of flight endurance of aerial networks. We will also discuss the novelty of our work into the perspective.

Coverage Problem and ABS Deployment: In [4], the authors address multiple cooperative coverage problem for more reliable and efficient aerial scenarios and propose multi-UAV coverage model based on the energy-efficient communication. First, the coverage probability from a given UAV is derived. Then, transmission power is determined to maximize coverage utility. Although the locations of users are known a priori, the user demands cannot be entirely predictable and this affects the coverage model. In [5], the authors focus on maximizing the coverage area of a single ABS under the constraint of transmission power. Then, the relationship between antenna gain and antenna beam angle is set up so that the flight altitude and coverage radius are adjusted according to beam angle. However, the provided solution cannot be optimal with multiple ABSs. In [6], the authors propose a deployment algorithm for UAV-BSs that maximizes the number of covered users with the minimum transmission power. In the horizontal dimension, the deployment problem is modeled as a circle placement problem and the results are confirmed with different user heterogeneity. However, the proposed solution is designed for 2D space. In [7], analysis and optimization of air-to-ground systems are researched. The authors derive optimal UAV altitude for reliable communication and maximum coverage area. However, energy is also an important factor that needs to be included into the working system for a reliable communication in aerial networks.

Maximizing Flight Endurance: Due to the battery constraints of ABSs, many research projects aim to minimize the duration of ABSs in reaching their designated locations so that hover time is maximized to achieve the assigned tasks. In [8], the authors deal with the deployment problem to transport UAVs in the shortest time. In addition, the computational complexity is analyzed and an optimal solution is proposed. However, this problem is simplified by focusing on predetermined clusters so that coverage area adjustment is not considered. In [9], survivability of the battery-operated aerial-terrestrial communication links is investigated to improve energy efficiency. However, aerial networks are constructed into the center of the target area, but this cannot be practical to maximize coverage area. In [10], throughput coverage is investigated by optimally placing UAVs for public safety communication after natural disaster. In contrast, the consumed energy of ABSs in our work is investigated and endurance is improved. In [11], flight time constraints of ABSs and the relationship between the hover time and bandwidth efficiency are investigated. First, given the maximum possible hover time, average data service is maximized. Then, given the load requirements of users, average hover time of ABSs is minimized to serve the users. The key difference between [11] and our work is that we schedule the operations of ABSs to improve the flight duration. In addition, we also jointly consider transition and hover time, both of which contribute to maximize endurance.

Path planning also provides some mechanisms to guarantee safe navigation of drones while avoiding collisions. In particular, with the usage area of drones in a wide range of applications, e.g., search and rescue operations, packet delivery service, traffic monitoring, drones can only achieve their missions by continuously updating the target region [12]. In order to maximize the collected data and reach the destination, path planning algorithms determine a path between source and destination node pairs. These algorithms include genetic algorithms [13], particle swarm optimization [14] or building a probability map [15] etc. The transition to the designated locations may face several uncertainties according to different path planning algorithms, such as obstacles, high computational complexity and unpredictability. This topic is not addressed in this paper. The main idea is to direct ABSs to the designated location along a flight path by minimizing the travel length.

In terms of the underlying algorithmic problems, the coverage problem in aerial networks is related to problems such as the set cover and sweep coverage problems. For example, the *set cover problem* looks for the fewest sets to cover a given set of points in the plane, which is NP-hard [16]. Our optimization problem can be seen as a geometric version, where the set size also depends on the height of the ABS [17]. Another related optimization problem considers a scenario, where a mobile drone/autonomous robot can continuously move to collect data from targets. By doing this, the robots aim to minimize so called sweep period for the given targets

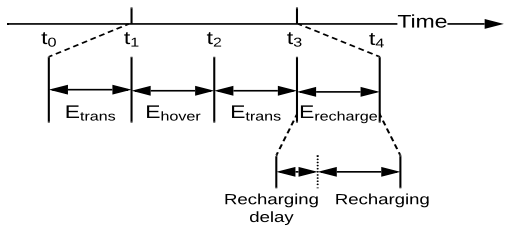

Fig. 2. ABS life cycle.

or reduce the trajectory length. This problem is referred to as the *sweep coverage problem* [18]. In both problems, the objective is to improve coverage utility and flight endurance by maximizing the energy efficiency. Following a similar objective, but considering a more general model, in this paper, we study the control of ABSs' operations with a centralized controller and find an energy-aware 3D deployment for ABSs to maximize flight endurance. Consequently, we provide useful guidelines to control ABSs' operations.

III. Network Architecture and Model

A. Network Model

We consider a square area of size Am^2 $(a(m)\times a(m))$ with M number of ABSs to cover the target area. Each ABS serves to the UEs, where UEs are uniformly distributed to the target area. An ABS recharges its battery at the replenishment station which is located on a mobile control station. The control station executes the *Optimal ABS Deployment*, *Minimization of Cost*, *Maximizing Endurance* and *Scheduling for Recharging* algorithms to manage the topology that will be detailed in the next section.

Each ABS can be in one of the following states. In addition, an ABS life cycle is shown in Fig. 2.

- Transiting State (s_{trans}): After the determination of the ABS locations, the consumed energy from initial location to the designated location and also from the designated location to the initial location are followed in this state. For mathematical denotation, we refer to the transition times as $t_1 - t_0$ and $t_3 - t_2$, respectively.
- Hovering State (s_{hover}): In this state, UEs remain connected with the ABSs and get service. We denote the hover time as $t_2 - t_1$.
- Recharging State $(s_{recharge})$: The ABS is on the replenishment station to recharge its battery.
- Sleeping State (s_{sleep}): If all replenishment stations are used by other ABSs and there is no available station for recharging, the ABS waits in this state. In addition, if no task is assigned to the ABS by the control station, the ABS is in this state until a new task is assigned.

Referring to [3], the mean value of the interference between ABSs, the coverage probability of the UE$_i$ is as follows:

$$\begin{aligned} P_{cov,i} &= \mathbb{P}\left[\frac{P_{r,i}}{N+I} \geq P_{threshold}\right] \\ &= P(LoS)_i \mathbb{P}\left[P_{r,i}(LoS) \geq P_{min}\right] + \\ &\quad P(NLoS)_i \mathbb{P}\left[P_{r,i}(NLoS) \geq P_{min}\right] \end{aligned} \quad (1)$$

where P_{min} is the minimum received power, $P_{min} = 10\log(NP_{threshold} + IP_{threshold})$, N is the noise power. We assume that noise power does not change over time for all receivers for simplicity and is equal to $-120dBm$. $P_{threshold}$ is the Signal-to-Interference and Noise (SINR) threshold ratio. This shows the necessary condition for connecting the UEs to ABS and I is the interference power received from the nearest ABS_k [3]:

$$I \approx P_t g(\varphi_k)\left[10^{\frac{-\mu_{LoS}}{10}} P_{LoS,k} + 10^{\frac{-\mu_{NLoS}}{10}} P_{NLoS,k}\right]\left(\frac{4\pi f_c d_k}{c}\right)^{-n} \quad (2)$$

where P_t is the transmission power of the ABS, $g(\varphi_k)$ is antenna gain, where $\approx 29000/\theta^2$ [3], θ is elevation angle, f_c is the carrier frequency, c is the speed of light. μ_{LoS} and μ_{NLoS} are the mean of shadow fading for *LoS* and *NLoS* and n is the path loss exponent $(n = 2)$.

The received signal from ABS for the UE$_i$ is as follows [19]-[20]:

$$P_{r,i}(dB) = \begin{cases} P_t + g - PL_{LoS,i} - \chi_{LoS}, & \text{for } \textit{LoS} \text{ link} \\ P_t + g - PL_{NLoS,i} - \chi_{NLoS}, & \text{for } \textit{NLoS} \text{ link} \end{cases} \quad (3)$$

where $\chi_{LoS} \sim N(\mu_{LoS}, \sigma^2_{LoS})$ and $\chi_{NLoS} \sim N(\mu_{NLoS}, \sigma^2_{NLoS})$ are the impact of shadowing caused by the obstacles with normal distribution. $(\mu_{LoS}, \sigma^2_{LoS})$ and $(\mu_{NLoS}, \sigma^2_{NLoS})$ are the mean and variance of shadow fading for LoS and NLoS, where $\sigma_{LoS}(\theta_j) = k_1\ exp(-k_2\theta_j)$ and $\sigma_{NLoS}(\theta_j) = g_1\ exp(-g_2\theta_j)$, respectively [3], [21]. The values of k_1, k_2, g_1, g_2 depend on the environment and they are constant. PL_i is the path loss. We use the path loss model for air-to-ground communication over urban environments. Each UE will have a *LoS* and *NLoS* link with some probabilities by connecting to the ABS. These probabilities depend on the location of UE and ABS, and environment. The *LoS* probability between the ABS and UE_i is given by [19], [20]:

$$P(LoS)_i = \frac{1}{1 + a \cdot exp(-b[\theta - a])} \quad (4)$$

where a and b are constant values that depend on the type of the environment (rural, urban etc). θ is the elevation angle and equals to $\theta = \frac{180}{\pi} arctan(\frac{h}{d_i})$. h and d_i represent the altitude of the ABS and distance between the ABS and UE$_i$. Note that the *NLoS* probability between the UE_i and ABS equals to $P(NLoS_i) = 1 - P(LoS_i)$. The path loss model for *LoS* and *NLoS* is given by [19]-[20]:

$$PL_i(dB) = \begin{cases} 20\log\left(\frac{4\pi f_c d_i}{c}\right) + \eta_{LoS}, & \text{for } \textit{LoS} \text{ link} \\ 20\log\left(\frac{4\pi f_c d_i}{c}\right) + \eta_{NLoS}, & \text{for } \textit{NLoS} \text{ link} \end{cases} \quad (5)$$

where η_{LoS} and η_{NLoS} are additional path loss coefficients and equal to 1 and 20, respectively for urban environments [21]. The parameters used in the paper are described in Table I.

B. Architectural Model

Fig. 3 shows the implementation of the control architecture. A *task* is defined for each ABS by the control station. An

TABLE I
PARAMETERS

Parameter	*Description*
M	Number of ABSs
A	The size of target area (Please note that a is the length of one side of the square)
$P_{cov,i}$	Coverage probability of UE_i
P_t	Transmission power of ABS
$P_{r,i}$	Received power by UE_i
P_{min}	Minimum received power
E_{max}	ABS battery capacity
N	Noise power
I	Interference received from the nearest ABS
$P(LoS)$	LoS probability
$P(NLoS)$	NLoS probability
$P_{threshold}$	SNIR threshold ratio
η	Path loss coefficient
$g(\varphi_k)$	Antenna gain
θ	Elevation angle
f_c	Carrier frequency
n	Path loss coefficient
ρ	Air density
m_d	ABS weight
m	ABS propeller
v_d	Average ABS speed
v_{max}	Maximum ABS speed

ABS is equipped with an RF receiver to receive control signals sent by the control station. The ABS initially follows its fixed task and no external communication is required. However, the defined task can be updated by the control station based on the network architecture. The *set up* block provides flight control information including hover location, coverage area, flight route and speed. The *critical controller* only includes the critical control functionality to provide an indication for energy consumption. In every time unit, control decisions are computed by the control station, and commands are sent to the ABSs. Once the consumed energy is known, the remaining energy information is evaluated based on the distance between the replenishment station and ABS so that timely and adaptive control decisions work in software. For this purpose, the *dynamics* block stabilizes the ABS. Rather than periodically triggering the controller of ABSs, we only run the set up block when an update is needed and the critical control is checked when the critical energy threshold is reached.

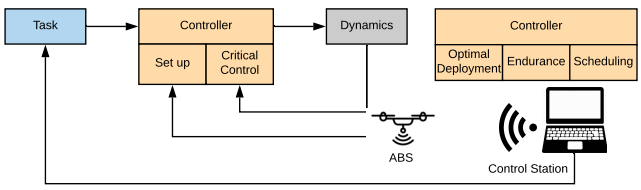

Fig. 3. Control architecture.

IV. *AirNet* SYSTEM

In this section, we provide an energy-aware solution, referred to as *AirNet* to deploy and schedule the ABSs and maximize the hover time with an endurance framework. We will describe *AirNet* in multiple steps. A general flow chart is shown in Fig. 4. As seen in the figure, we determine the locations of ABSs in Alg. 1. After ABS deployment, we

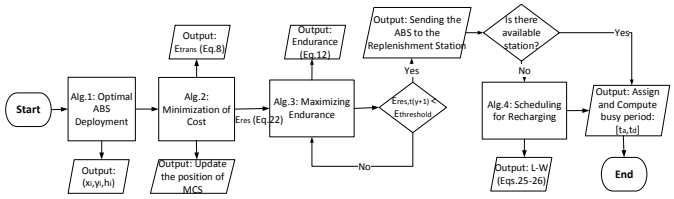

Fig. 4. *AirNet* flow chart.

calculate the consumed and residual energy, and update the location of the mobile control station in Alg. 2. In order to maximize flight endurance, we propose Alg. 3. After the ABS's battery is at a critical level, we schedule the ABS operations for recharging in Alg. 4.

A. Optimal ABS Deployment

We first focus on a single ABS deployment to cover the target area. To simplify the presentation, as shown in Fig. 5, the target area is divided into grid cells. Here, the number of UEs can vary from cell to cell. Our main idea for this demonstration is to observe the density of the UEs in the target area. If a cell includes a number of UEs, the cell is marked as '1'. Otherwise, it is marked as '0' to show the empty cell. This means that there is no UE in this cell. Depending on the altitude of the ABS, the coverage area also changes. Here, we define $R_{cluster}$ so that UE can only be connected to the ABS in this cluster. At the initial phase, according to the UE locations, we find the center of minimum radius to cover maximum number of UEs. Mathematically, with the *Chebyshev Center* formulation, the problem can be written as follows:

$$min_{\mathbf{x},R_{cluster}} R_{cluster} \tag{6}$$

subject to

$$\left\|\mathbf{x} - UE_i\right\| \leq R_{cluster}, \quad i = 1, 2, .., U. \tag{7}$$

where $\mathbf{x}$ is the center point of the cluster and U is the number of UEs.

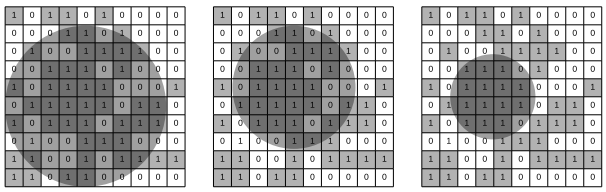

Fig. 5. Adjustment of coverage area with a single ABS.

However, it may not be effective when the whole target area is only covered by a single ABS since each UE cannot have a good signal quality with the given transmission power. Therefore, we first define $R_{cluster}$ with h_{max} and, then check the received power of the UEs with the SINR threshold value as given in Eq. 1. At each step, we repeat this process with $h^* = (h_{min} + h_{max})/2$ until the solution is feasible. Then, we update the coverage area radius with Alg. 1 as shown in the Fig. 5. According to [22], the height of the small

unmanned aircraft cannot be higher than 400 feet above ground level. Thus, under the SINR connection model, the altitude is adjusted between $h_{min} = 20m$ and $h_{max} = 100m$ to determine the strength of the received signal from the desired ABS and avoid the interference caused by other ABSs and the noise power. Optimal ABS altitude enables maximum coverage area with a minimum required transmission power.

Algorithm 1 Optimal ABS Deployment

1: $Given : h_{min} \leq h^*,\ h_{max} \geq h^*$
2: $Tolerance : \left[\frac{P_{r,i}}{N+I} \geq P_{threshold}\right]$
3: **repeat**
4: (1) $h^* = (h_{min} + h_{max})/2$
5: Solve the feasibility problem (1)
6: **if** (1) is feasible **then** $h_{max} = h^*$
7: **else** $h_{min} = h^*$
8: **until** $\forall$ UE$_i \in R_{cluster}$ $\left[\frac{P_{r,i}}{N+I} \geq P_{threshold}\right]$

Alg. 1 solves the deployment problem with the computational complexity of $O(n \log n)$. The analysis is performed for each ABS. We first note that h^* produced by Alg. 1 is feasible. Otherwise, Alg. 1 ends when $\left[\frac{P_{r,i}}{N+I} \geq P_{threshold}\right]$ for each $UE_i \in R_{cluster}$. Since we adjust the altitude between h_{min} and h_{max} for each ABS, we start with maximum altitude to cover the UEs as much as possible. Suppose we have the solution $x = (x_1, x_2, ..x_m)$, $y = (y_1, y_2, ..y_m)$ with optimal altitude $h = (h_1, h_2, ..h_m)$. With the defined $R_{cluster}$ as given in Eq. 6, Line 2 is checked for each $UE_i \in R_{j,cluster}$. This is repeated for each deployed ABS.

We assume that each ABS starts with maximum and identical energy capacity, E_{max}. The consumed energy from initial location $(0, 0, 0)$ to the designated location (x_j, y_j, z_j) will directly affect the lifetime of the ABS since the coverage utility depends on the available energy at the ABS. We define a cost parameter, which is the consumed transition energy from the initial position to the designated position for ABSs. The consumed transition energy is given in Eq. 8 [23]-[24]:

$$E_{trans} = \left(\frac{P_{full} - P_s}{v_{max}} v_d + P_s\right)(t_1 - t_0) \tag{8}$$

where v_d is the constant ABS speed during the trip, v_{max} is the maximum speed of the ABS. P_{full} is the hardware power level when the ABS is moving at full speed. P_s is the power level when the ABS stops in a fixed position $(v_d = 0)$. $t_1 - t_0$ is the transition time from initial location to the designated location. The optimization problem aims to minimize the consumed transition energy from the deployed location to the initial location for the ABSs as given in Eq. 9.

$$\min \sum_{j=1}^{M} \left[\left(\frac{P_{full} - P_s}{v_{max}} v_d + P_s\right)\vartheta_j\right](t_3 - t_2) \tag{9}$$

subject to

$$C_1 : \vartheta_j \in \{0, 1\} \quad j \in M \tag{10}$$

$$C_2 : \sum_{j=1}^{M} a_{ij}\vartheta_j \leq 1 \quad for\ each\ UE \tag{11}$$

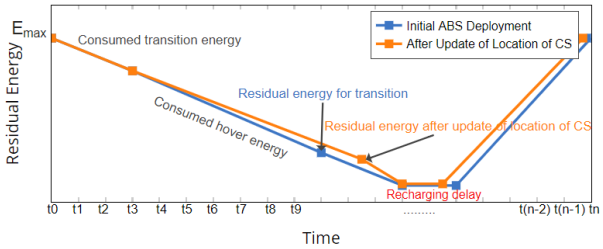

Fig. 6. Residual energy for two different cases.

where ϑ_j is a binary variable to follow active ABSs. C_2 indicates that a UE cannot get service from more than one ABS. $a_{ij} = 1$ if UE_i is covered by ABS_j, otherwise $a_{ij} = 0$. M is the number of ABSs. $(t_3 - t_2)$ is the transition time, where $t_3 - t_2 = d/v_d$, where d is the flying distance with a constant velocity.

As seen in Fig. 6, the duty cycle of an ABS starts with the transition. The residual energy will decrease over time so that after ABS deployment, we focus on decreasing transition energy from designated location to the replenishment station as given in Eq. 9. To do this, we propose to update the location of the control station while guaranteeing the minimization of cost with Alg. 2. Here, we also aim to cover a maximum number of UEs when the number of ABSs is limited. While the maximum coverage problem is NP-hard under the limited ABS (Line 2-5), we can obtain a greedy approximation factor of $1 - \frac{1}{e}$, which is explained in Appendix A [25].

Algorithm 2 Minimization of Cost

1: Initialize: $E_{trans,j} \leftarrow \emptyset$ and $U \leftarrow X$ (U is the set of uncovered UEs and X is the finite set of UEs)
2: **while** $\forall$ ABS_j is deployed **do**
3: Let S be a set such that $|S \cap U|$ is maximized (S covers the largest number of UEs in U)
4: $U \leftarrow U \backslash S$ (remove from UEs in U that are covered by ABS_j)
5: **end while**
6: $DemandAwareReconfiguration()$ // cf Section IV.B
7: Update (x, y) position of MCS as $(x, y) = \frac{S_{1,x,y},\ldots,S_{M,x,y}}{M}$ ($S_{1,x,y}$ is the center point of set S_1)
8: **for** $j \leftarrow 1$ to M **do**
9: Calculate $E_{trans,j}$ with Eq. 8
10: **end for**
11: **return** $E_{trans,j}$

While a detailed evaluation is given in the next section, to get some intuition on the effectiveness of the algorithms, we first conduct simple experiments. This is performed in MATLAB for an environment with one and two ABSs, respectively. Then, the commands are tested with MAVProxy 1.5.0 that runs on SITL (Software In The Loop) ArduPilot simulator using Cygwin [26]. We observe the coverage areas for a better understanding of the network performance. Fig. 7 shows the deployment of one ABS with $(10^{-4} UEs/m^2)$ and two ABSs with $(2x10^{-4} UEs/m^2)$, respectively.

With different UE densities, we show the relationship between the coverage radius, $R_{cluster}$ and optimal altitude

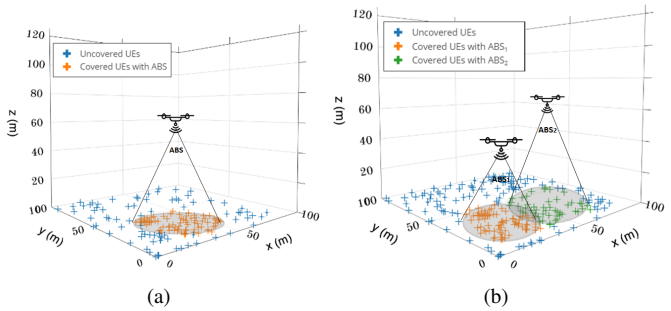

(a) (b)

Fig. 7. (a) Coverage area with single ABS $(10^{-4}UEs/m^2)$ (b) Coverage areas with 2 ABSs $(2x10^{-4}UEs/m^2)$.

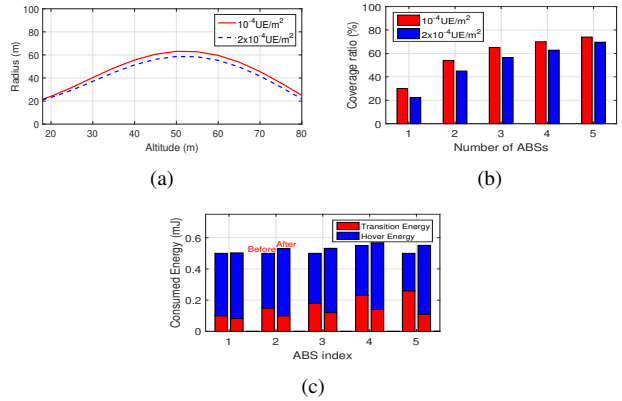

(a) (b)

(c)

Fig. 8. (a) The relationship between coverage radius, $R_{cluster}$ and altitude (b) Coverage ratio with increasing number of ABSs (c) Consumed transition and hover energy before the first ABS deployment and after the update of location of control station.

in Fig. 8(a). After the optimal height is obtained, as the height of ABS increases, the coverage radius will decrease because of the SINR. We also illustrate the coverage ratio with the increasing number of ABSs for $(10^{-4}UEs/m^2)$ and $(2x10^{-4}UEs/m^2)$ densities in Fig. 8(b). Then, we compare two different scenarios in Fig. 8(c) with 5 ABSs. At first, we deploy ABSs and calculate the consumed transition and hover energy with Eqs. 8 and 21, respectively. Then, we update the location of control station as explained in Alg. 2 and obtain average 14% degradation in terms of the consumed transition energy. This will increase the hover time of ABSs.

B. Demand-Aware Reconfiguration

The key feature in our approach is that *AirNet* supports demand-aware operation. User demand can vary over time in an unpredictable way, which leads us to analyze time-varying user demand. Satisfying the dynamic user demand requires reconfiguration in an online manner.

To achieve this, we check the traffic load of each ABS for the demand-aware reconfiguration. Here, we only focus on overlapping areas since coverage areas and the position of ABSs can be reconfigured to satisfy users' demands. Overlapping areas are the regions where UEs can connect $k-$ABS since this region is covered by $k-$ABS. Therefore, we assign the UEs in the overlapping areas to the ABS which has the low traffic load.

Traffic demands are kept in a *demand matrix*, D, for each time t_y, where $t_1 < t_y < t_2$. An entry $D_{(i,j)}$ in D is the demand from UE_i to ABS_j. It is assumed that the demands have variable packet size, L_i with power law distribution and their arrival rate, λ_i with Poisson distribution. Since user demand can vary with different types of applications, there should be a fair resource allocation among the traffic demands to satisfy users' QoS. Here, we consider the well-known D'Hondt Algorithm [27]-[28] (seat allocation) to assign Resource Blocks (RB) to the UEs and determine 'fair' allocation.

TABLE II
SIMULATION FOR THE ALLOCATION 9 RBS WITH 3 UES.

Order of RB Allocation	Divisor (UE_1)	Average (UE_1)	Divisor (UE_2)	Average (UE_2)	Divisor (UE_3)	Average (UE_3)
1st	1	**10**	1	6	1	2
2nd	2	5	1	**6**	1	2
3rd	2	**5**	2	3	1	2
4th	3	**3.33**	2	3	1	2
5th	4	2.5	2	**3**	1	2
6th	4	**2.5**	3	2	1	2
7-9th	5	**2**	3	**2**	1	**2**
-	6	1.667	4	1.5	2	1
Total		**5**		**3**		**1**

To explain the algorithmic method, we provide an example and show the implemented steps in Table II. Assume that there are 9 unassigned RBs and 3 UEs with 10, 6 and 2 demands as seen in the $1st$ row. In this case, the existing RBs will not supply all traffic demands. All demands are listed for determining a fair allocation. There is also a divisor parameter, which initially is set to 1 for each UE. The $1st$ RB is allocated to UE_1 because of the highest demand. Then, the divisor is first incremented for UE_1 and then, the average demand is calculated as $\frac{demand}{divisor}$ as seen in the $2nd$ row. The divisor will not change for UE_2 and UE_3. In the next step, the $2nd$ RB is allocated to UE_2 since UE_2 has now the highest average demand. Similarly, the divisor is first incremented for UE_2 and then, the average demand is calculated as $\frac{demand}{divisor}$ in the $3rd$ row. These processes continue until all resources are allocated, (i.e. $\lambda_i \leftarrow \lambda_i/2$, $\lambda_i \leftarrow \lambda_i/3$, and so on). In the end, UE_1, UE_2, and UE_3 allocate 5, 3, 1 RBs, respectively, as seen in the *Total* row in the table. As a result, each division produces an average, and the 'highest average demand' is awarded to the available RB, until all RBs have been allocated.

C. Endurance Framework

Energy consumption of ABSs is of paramount importance for aerial networks since it directly affects the endurance and limits the network lifetime. In general, the consumed energy of an ABS is based on (i) transition power, P_{trans}, from initial location to the designated location and vice versa, (ii) hover power, P_{hov}, to serve UEs and (iii) communication power, P_{com}. Minimizing each of them can help to extend ABSs' lifetime.

With this purpose, each ABS independently maximizes the endurance (Υ). It is defined as the flight duration in the hovering state so that a higher hover energy leads a higher endurance. The problem is considered as follows:

$$\Upsilon = \frac{E_{max} - [E_{trans_{t_1-t_0}} + E_{trans_{t_3-t_2}}]}{P_{hov}} \quad (12)$$

Accordingly, the optimization problem is to maximize the endurance as given in Eq. 13.

$$\max_{h_{min} \leq h^* \leq h_{max}, R_{cluster}} \Upsilon_j \quad \forall j \in M \tag{13}$$

subject to

$$C_1 : E_{res,t_y} \geq \int_{t_2}^{t_3} P_{trans} dt \tag{14}$$

$$C_2 : \theta_j \in [\theta_{min} - \theta_{max}] \tag{15}$$

$$C_3 : a_{ij,t_y} \in \{0,1\} \quad (1 \leq i \leq N), (1 \leq j \leq M), (t_2 \leq t_y \leq t_3) \tag{16}$$

$$C_4 : \sum_{j=1}^{M} a_{ij,t} \leq 1 \tag{17}$$

where C_1 is the residual energy constraint, which will be detailed below. C_2 limits the relation between the altitude and coverage radius, where θ is the angle formed by the center of one of the circles and the points of intersection of the circles. C_3 states that if ABS serves the UE in the designated time slot t_y, then $a_{ij,t_y} = 1$, otherwise $a_{ij,t_y} = 0$. Additionally, C_4 states that a UE cannot get service from more than one ABS in the designated time slot.

Total energy capacity of an ABS is given in Eq. 18:

$$E_{max} = \int_{t_0}^{t_1} P_{trans} dt + \int_{t_1}^{t_2} [P_{hov} + P_{com}] dt + \int_{t_2}^{t_3} P_{trans} dt \tag{18}$$

Accordingly, the hover power is given in Eq. 19:

$$P_{hov} = \frac{F^{3/2}}{\sqrt{2\rho A}} \tag{19}$$

where $F = m_d g$, m_d is the ABS weight (kg), g is the earth gravity (m/s^2), and $A = \pi r^2 m$, r is the radius of ABS's propellers and m is the number of drone's propellers. ρ is the air density (kg/m^3).

$$P_{hov} = \frac{(m_d g)^{3/2}}{\sqrt{2\pi r^2 m \rho}} \tag{20}$$

and

$$E_{hov} = \int_{t_1}^{t_2} \frac{(m_d g)^{3/2}}{\sqrt{2\pi r^2 m \rho}} dt \tag{21}$$

Transition energy is given in Eq. 8 and the power consumption for the communication (P_{com}) is neglected to reduce the computation complexity.

E_{res,t_y} is the residual energy level of the ABS at time t_y and E_{con,t_y} is the consumed energy at time t_y, where $t_1 < t_y < t_2$.

$$E_{res,t_y} = E_{max} - E_{con,t_y} \tag{22}$$

and

$$E_{con,t_y} = \int_{t_0}^{t_1} P_{trans} dt + \int_{t_1}^{t_y} P_{hov} dt \tag{23}$$

$$E_{res,t_y} \geq \int_{t_2}^{t_3} P_{trans} dt \tag{24}$$

In order to manage ABSs, we introduce Alg. 3. The principle is to track the residual energies of ABSs in each time slot and give a decision for recharging. After the decision to recharge, we calculate the consumed energy as given in Eq. 23, thereby, the lower the consumed energy, the quicker the charging time. Then, each ABS is either assigned to one of the replenishment stations or programmed to the sleeping state. The control station executes Lines 2-3 of the Alg. 3 for each ABS per discrete time slot and this takes $O(1)$ operations. Similarly, Lines 4-7 are $O(1)$. Thus, the total complexity is $O(n)$ operations per discrete time.

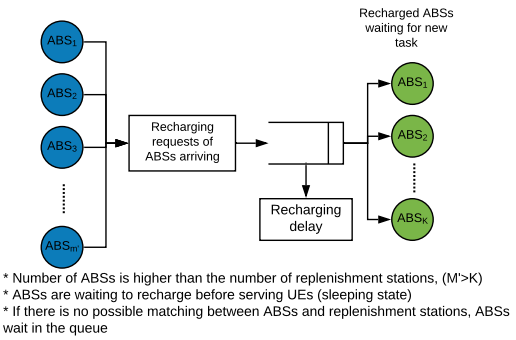

Fig. 9. Recharging requests of ABSs.

Algorithm 3 Maximizing Endurance

1: **for** $j \leftarrow 1$ to M **do**
2: $E_{res,t_{y+1}} \leftarrow$ *compute* $\forall j \in M$
3: $E_{threshold} \leftarrow \int_{t_2}^{t_3} P_{trans}(t)$ //Please note that the location of control station is updated in Alg. 2
4: **if** $E_{res,t_{y+1}} < E_{threshold}$ **then**
5: Schedule for charging
6: $w_j \leftarrow E_{con,t_y}$
7: **end if**
8: **end for**
9: Sort ABS according to w_j in ascending order
10: Select the ABSs in order for recharging

D. Scheduling between ABSs and Replenishment Stations

In Eq. 24, the controller follows the residual energy after the ABS is at the hovering state and accordingly, gives a decision for recharging based on the threshold energy level. Please note that threshold energy level is different for each ABS and calculated in Alg. 3. If the number of ABSs that needs to be recharged is more than the number of available replenishment stations, there should be a scheduling mechanism. In this case, these ABSs wait in the sleeping state to be recharged as illustrated in Fig. 9. Thus, in the proposed model, the controller presents a strategy to schedule the ABSs' operations.

With the proposed approach, the control station starts scheduling with the first arrival of ABS to the replenishment stations and, then updates the system when a new arrival or departure occurs with Eqs. 25-26.

$$L = \sum_{n=1}^{T} \tau(t_n - t_{n-1})/T \tag{25}$$

and

$$W = \sum_{t_a, t_d \in T}^{T} [t_d - t_a]/M' \tag{26}$$

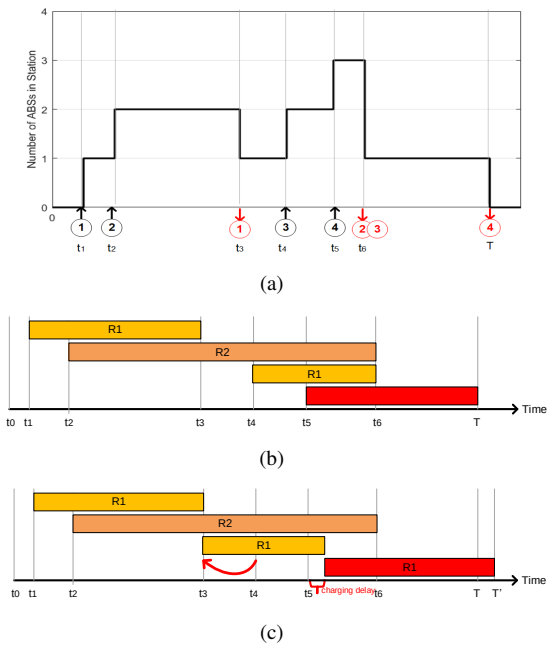

Fig. 10. (a) Illustration of busy periods of replenishment stations (b) Before scheduling (c) After scheduling.

where L and W are the mean number of the ABSs and mean charging time (min) in the replenishment station, respectively. τ and M' represent the number of ABSs at time t and the total number of arrivals over the time period $[0, T]$, respectively. t_a and t_d are the arrival and departure times of ABSs in the system. This also shows the charging time of an ABS, where $[t_d - t_a](min) = CE_{con}/I_c E_{max}$, C (in mAh) is the capacity of the battery and I_c (in Ampere) is the current of the charge.

For example, consider the illustration in Fig. 10(a), the number of the ABSs that arrives to the station for recharging over the time period $[0, T]$ is $M' = 4$. Black circles show the arrivals and red circles show the departures. L and W parameters are given in Eqs. 27-28 [29].

$$\begin{aligned} L &= \big[1(t_2 - t_1) + 2(t_3 - t_2) + 1(t_4 - t_3) + 2(t_5 - t_4) \\ &\quad +3(t_6 - t_5) + 1(T - t_6)\big]/T \\ &= \big[T + 2t_6 - t_5 - t_4 + t_3 - t_2 - t_1\big]/T \end{aligned} \tag{27}$$

$$\begin{aligned} W &= \big[(t_3 - t_1) + (t_6 - t_2) + (t_6 - t_4) + (T - t_5)\big]/K \\ &= \big[T + 2t_6 - t_5 - t_4 + t_3 - t_2 - t_1\big]/4 \end{aligned} \tag{28}$$

However, if we assume that the number of replenishment stations is equal to $R = 2$, as seen in Fig. 10(b), it cannot be possible to recharge ABS_4 at time t_5 so that ABS_4 waits in the sleeping state until t_6. Thus, we propose a scheduling mechanism to minimize the waiting times of ABSs for recharging under the assumption of the limited number of replenishment stations as given in Alg. 4. Alg. 4 runs with the first arrival and tracks the busy periods of the replenishment stations ($[t_a, t_d]$) over the time period $[0, T]$. If there is no available station, then the busy periods are computed in the case of early arrival (Lines 7-13) and accordingly, the task is updated by the control station.

As seen in Fig. 10(c), the task of ABS_3 is updated and then ABS_3 is ready for recharging at time t_3 so that ABS_4 is now scheduled after the departure of ABS_3. Another approach could be to update the task of ABS_2. However, in this case, we assume that $t_6 - t_4 + t_3 < t_6 - t_2 + t_1$. This is controlled in Alg. 4. Let us now discuss the computational complexity of implementing the Alg. 4. Each ABS that arrives to the station for recharging executes this procedure with $O(n)$ operations. Each line between 3 to 6 is accomplished with $O(1)$ operation per discrete time step. For the worst case scenario, all ABSs wait for recharging and replenishment stations are busy. The total complexity is $O(n)$ operations between lines $8 - 10$. Similarly, each line between 11 to 13 is accomplished with $O(1)$ operation per discrete time step. Thus, the total complexity is $O(n^2)$ operations.

Algorithm 4 Scheduling for Recharging

1: Sort ABSs by arrival time over the time period [0,T] so that $t_{a1} \leq t_{a2} \leq .... \leq t_{aK}$
2: **for** $j \leftarrow 1$ to M' **do**
3: **if** ABS_j is compatible with a station r **then**
4: Schedule ABS_j to the station r
5: $[t_{aj}, t_{dj}] \leftarrow$ *compute busy periods for* $r \in R$
6: $t(r) \leftarrow t_{dj}$ // station r is busy until t_{dj}
7: **else**
8: **for** $r \leftarrow 1$ to R **do**
9: new $(t(r)^*_{dj}) = t(r)_{dj} + t(r)_{aj-1} - t(r)_{aj}$
10: **end for**
11: Select min(updated $(t(r)^*_{dj})$)
12: Update the task of ABS_j*
13: Allocate the station r at first available $(t(r)^*_{dj})$ and schedule ABS_j to the defined station
14: **end if**
15: **end for**

V. Performance Evaluation

In this section, we extensively evaluate the effectiveness of *AirNet*. To analyze this, we first consider four different schemes to deploy ABSs under the constraint of limited number of ABSs: (i) Random ABS deployment (ii) ABS deployment to the locations of damaged BS (iii) Set cover approach (iv) Energy-aware ABS deployment. Then, we verify the benefits of an optimized scheduling of the ABSs' visits to the replenishment stations.

A. Simulation Setup

First, the proposed model has been implemented in MATLAB 2018a. Then, Cygwin software is used for the ABS control with Software in the Loop (STIL) ArduPilot simulator [26] and MAVProxy 1.5.0 with C++ compiler.

In our simulation, we consider ABS-based communication for urban environment over $2GHz$ carrier frequency with $a = 4.2$ and $b = 8$ with $k_1 = 10.39$, $k_2 = 0.05$, $g_1 = 29.06$, $g_2 = 0.03$ [3], [21]. UEs are uniformly distributed with $\lambda_u = 4x10^{-2} UEs/m^2$ in $50x50$ cells, where the length of each cell is $20m$. We assume that ABS transmission power is $P_t = 24dBm$, battery capacity is $2x10^4 mAh$, average (v_d) and maximum speed (v_{max}) are $10m/s$ and $20m/s$, respectively. An ABS transmits at power level $P_{full} = 5W$ with full speed and when $v_d = 0$, $P_s = 0$. It is assumed that ABS weight is $m_d = 650g$ with $m = 4$ propellers, air density is $\rho = 1.125kg/m^3$ and charge rate current is $2.4A$.

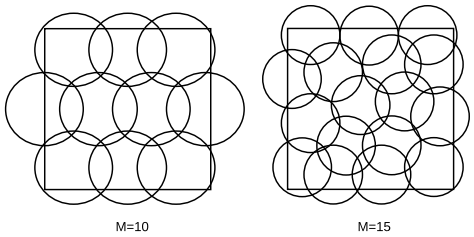

Fig. 11. Covering a given target area with M=10 ($R_{cluster} = 0.2182a(m)$) and M=15 ($R_{cluster} = 0.1796a(m)$).

B. Benefits of Energy-Efficient Deployment

As the baseline ABS deployment comparison, Fig. 12 shows 4 different approaches with 10 ABSs as follows.

- *Random ABS deployment:* We randomly deploy the ABSs to the target area with the same coverage radius ($R_{cluster} = 50m$).
- *ABS deployment to the locations of damaged BS:* We deploy the ABSs to the locations of damaged BS at fixed height ($h = 60m$).
- *Set cover approach:* As a baseline comparison, we analyze the study in [3]. In this scheme [3], the circle packing approach is considered to cover a given target area and the authors compute the coverage utility and coverage radius. We made some changes in this study to apply our scenario. First, we consider the target region as a square area instead of a circular area. Then, we focus on covering the entire target area. To exemplify this, Fig. 11 is given with 10 and 15 ABSs. As seen in the figure, when the required number of ABSs changes, the coverage radius shows a difference. By considering this approach, we create the circles to cover all target area with the same radius ($R_{cluster} = 50m$) since [3] considers the fixed circles. Then, we consider the set cover problem that selects the sets with maximum number of UEs under the constraint of the limited number of ABSs.
- *Energy-aware ABS deployment: AirNet*, which was presented in the previous section.

In Fig. 12, we set the number of ABSs as 10 and show the coverage areas for 4 different approaches, respectively. First, we randomly deploy the ABSs in Fig. 12(a) and analyze coverage utility for the target area. Then, in Fig. 12(b), it is assumed that terrestrial BSs are located with the distance of $200m$ in the target area and we deploy ABSs to these locations at the fixed height, $h = 60m$. Since it is not possible to cover all UEs within the coverage area of a terrestrial BS, we deploy the ABSs to maximize the number of covered UEs. At each step, we select the sets which have maximum number of UEs. In Fig. 12(c), we mainly focus on the prior work [3] as a baseline that uses ABSs to provide wireless coverage in a given geographical area. We initially consider coverage problem with circles, $R_{cluster} = 50m$ and we define the required number of circles to cover target area as explained in [30]. Then, we focus on the set cover problem since we assume that the number of ABSs is limited and we select the circles that maximize the number of covered UEs.

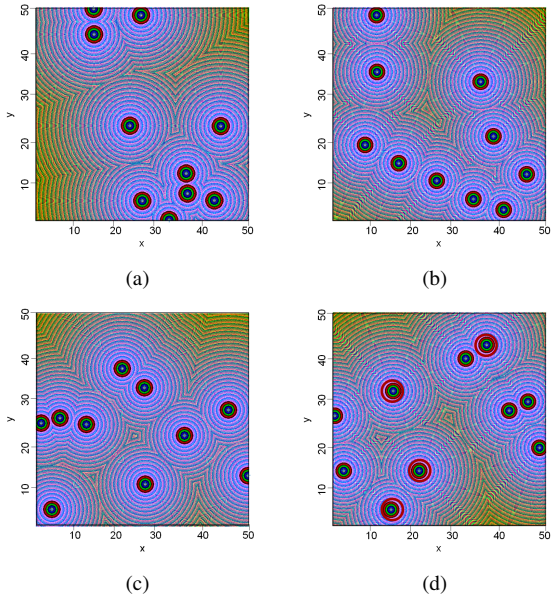

Fig. 12. ABS deployment for different schemes with 10 ABSs (a) Random ABS deployment (b) ABS deployment to the locations of damaged BS (c) Set cover approach (d) Energy-aware ABS deployment.

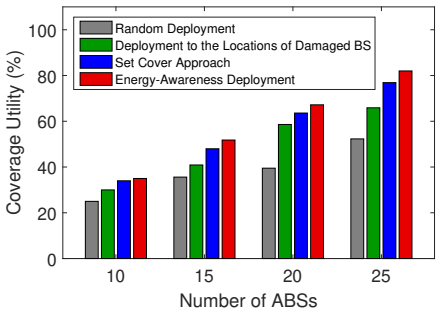

Fig. 13. Coverage utility for 4 different schemes.

Finally, in Fig. 12(d), we show the proposed energy-aware ABS deployment and evaluate the results. Please note that after ABS deployment, the comparisons will show how the algorithms reflect the performance evaluation in terms of the coverage utility, consumed transition energy, throughput, and recharging delay.

Fig. 13 shows the coverage utility with the deployment of 10, 15, 20, and 25 ABSs. Coverage utility is the ratio of covered UEs to the all UEs. We see that when the number of ABSs increases, *AirNet* provides the best results, it also outperforms to the set cover approach. Energy-aware deployment adjusts maximum coverage area with the minimum required transmission power in Alg. 1 and it enables average 24% and 3.72% increase in the coverage utility when compared to the random and set cover approach [3], respectively. As seen in the figure, random and deployment to the locations of damaged BS are not directly applicable for a potential solution in the mission critical environments.

After energy-aware ABS deployment, we investigate the consumed transition energy for 10 ABSs in Fig. 14. The transition energy from control station to the designated loca-

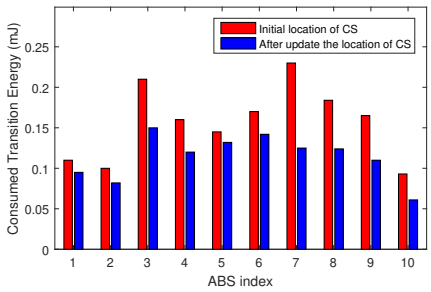

Fig. 14. Consumed transition energy of individual ABSs.

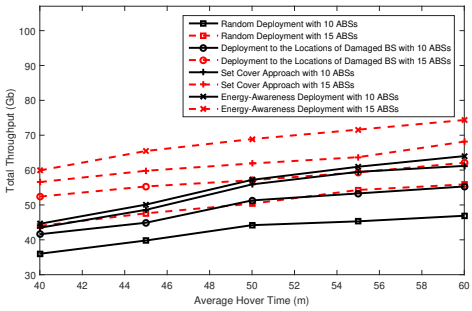

Fig. 15. Average hover time w.r.t. total throughput

tion $\left(E_{trans} = \int_{t_0}^{t_1} P_{trans} dt\right)$ and designated location to the control station for recharging $\left(E_{trans} = \int_{t_2}^{t_3} P_{trans} dt\right)$ are analyzed, where Eq. 8 gives the details. Initially, the control station was located at (0,0) in the axes and ABSs are directed to the designated locations (x_j, y_j, z_j). Then, the position of control station is adaptively updated with Alg. 2 and we compute the consumed transition energy for each ABSs so that the hover time is increased 8% in the aerial networks.

C. Demand-Aware Reconfiguration

Since user demand can vary over time in an unpredictable way, this motivates us to analyze the demands as variable and also not known. Therefore, we assume that the packet arrival rate is $\lambda = 60$ *packets/sec* with Poisson distribution and the packet size distribution has the power law behavior with the mean 1100 bytes to design an efficient traffic model. Power-law distribution is used to characterize the equilibrium of the users' demands. Under the packet size distribution and availability of the existing resources, demand-aware reconfiguration enables a fair resource allocation. In this respect, in Fig. 15, we show the total throughput with respect to the average hover time with 10 and 15 ABSs. More importantly, it is shown that when the number of ABSs is increased, the proposed model enables significant improvement thanks to demand-aware reconfiguration and the rate at which the throughput does not increase the same rate for different schemes.

D. Benefits of Scheduling

Under the assumption of the limited number of replenishment stations, in order to observe the benefits of the scheduling mechanism, Fig. 16 shows the normalized recharging delay

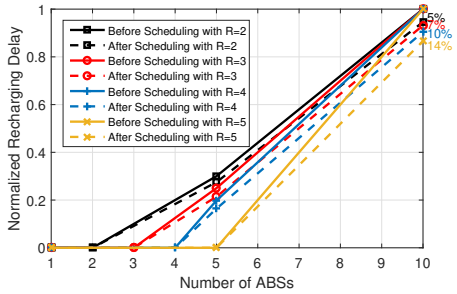

Fig. 16. Normalized recharging delay before scheduling and after scheduling with different number of replenishment station.

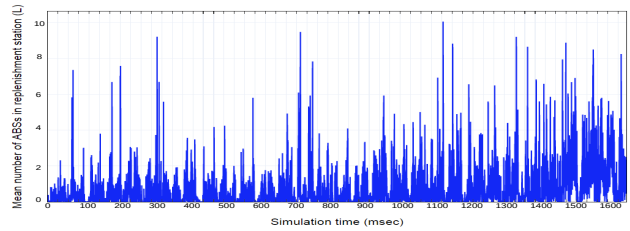

(a)

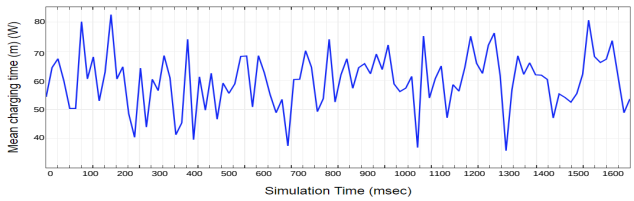

(b)

Fig. 17. (a) Mean number of ABSs and (b) Mean charging time in the replenishment station.

before and after scheduling approaches according to the different number of replenishment stations. Recharging delay is defined as the waiting time before being recharged. In order to provide a clearer illustration, recharging delay is independently normalized for different number of stations. The results are obtained with respect to the increasing number of ABSs. Note that we only focus on ABSs that wait in the recharging state. The benefit of providing a scheduling between the ABSs and stations is seen from the figure, when the number of stations increases, the results indeed outperform greatly. Thus, to obtain the results for the scheduling mechanism, we first compute the mean number of ABSs and mean charging time in the replenishment station over the simulation time as shown in Figs. 17(a)-17(b) with Eqs. 25-26, respectively so that we can evaluate the recharging delay. In Fig. 17, we assume that there are 4 stations with respect to the changing number of ABSs. As expected, when the number of ABSs that needs to be recharged is higher than 4, the construction of the scheduling mechanism will be very useful to guarantee a better network management.

Next, we demonstrate the Probability Density Function (PDF) of recharging delay for 2, 3, 4 and 5 replenishment stations with one ABS in Fig. 18. Note that in order to obtain reliable simulation estimates, we set the number of ABSs to 8. The range of recharging delay is calculated based

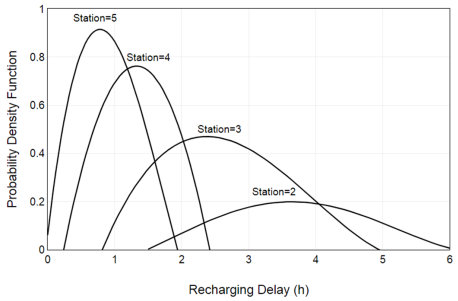

Fig. 18. PDF of the recharging delay for one ABS. The number of replenishment station equals to 5, 4, 3 and 2. The number of waiting ABSs set to 8.

on the waiting time before being recharged, as the available stations are less than the number of the waiting ABSs in the recharging state. Then, the total recharging delay curve is obtained by accumulative stacking. As seen in the Fig. 18, when the number of stations decreases, for each ABS, it is more probable to wait. As the number of stations increases from 2 to 5, the value of the mean waiting time before being recharged approximately drops from 3.4 to $0.94h$. This implies that the increase on the number of stations will cause a significant decrease in the recharging delay and this mean value is improved with the proposed scheduling approach.

VI. Conclusion & Future Work

In this paper, we presented and evaluated *AirNet*, an energy-aware ABS deployment and scheduling mechanism accounting for replenishment stations. We addressed the problem of ABS deployment to maximize the number of covered UEs in an online manner. In particular, AirNet's operation is demand-aware and accounts for the time-varying user requests. We also demonstrated, using an energy model, how an efficient algorithm can increase the flight endurance. Furthermore, we presented a scheduling algorithm for battery recharging under the constraint of a limited number of replenishment stations. Our simulations also confirm the effectiveness of the proposed algorithms in terms of the user coverage and flight endurance. In particular, our results indicate that *AirNet* can achieve 24% improvement in the user coverage and 8% extension in the flight endurance.

We see our work as a first step and believe that it opens several interesting avenues for the future research. In particular, we so far assumed a relatively simple model for the to-be-covered area, and it would be interesting to investigate more complex scenarios, e.g., due to mountains or other obstructions. It would also be interesting to consider the use of randomized algorithms.

Appendix A
Proof of Approximation

In Alg. 2, we initially select M-sets that maximize the number of covered UEs. Here, OPT shows the optimal solution to maximize the number of covered UEs. Let us denote a_i as the number of newly covered UEs, b_i as the total number of UEs and c_i as the number of uncovered UEs at the i_{th} iteration so that $b_i = \sum_{j=1}^{i} a_j$ and $c_i = OPT - b_i$ [25].

The number of newly covered UEs at the $(i+1)_{th}$ iteration is equal to or greater than $1/M$ of the number of uncovered UEs after i_{th} iteration such that $a_{i+1} \geq \frac{c_i}{M}$.

Lemma: $c_{i+1} \leq (1 - \frac{1}{M})^{i+1}.OPT$

Proof: By induction, we give the steps for $i = 0$.

$$\begin{aligned} c_1 &\leq \left(1 - \frac{1}{M}\right) OPT \\ OPT - b_1 &\leq OPT - OPT\ \frac{1}{M} \\ b_1 &\geq OPT\ \frac{1}{M} \\ a_1 &\geq OPT\ \frac{1}{M} \\ a_1 &\geq c_0\ \frac{1}{M} \end{aligned} \tag{29}$$

Then, we know $a_1 \geq c_0 \frac{1}{M}$ for $i = 0$. Assume $c_i \leq (1 - \frac{1}{M})^i\ OPT$ is true, we show that $c_{i+1} \leq (1 - \frac{1}{M})^{i+1}\ OPT$ is true.

$$\begin{aligned} c_{i+1} &= c_i - a_{i+1} \\ c_{i+1} &\leq c_i - \frac{c_i}{M} \\ c_{i+1} &\leq c_i\ (\frac{1}{M}) \\ c_{i+1} &\leq (\frac{1}{M})^i\ OPT\ (1 - \frac{1}{k}) \\ c_{i+1} &\leq (\frac{1}{M})^{i+1}\ OPT \end{aligned} \tag{30}$$

Theorem: A greedy algorithm achieves a $(1 - \frac{1}{e})$ approximation factor.

Proof: By Lemma 1, we know that $c_M \leq (1 - \frac{1}{M})^M\ OPT$. Then, $(1 - \frac{1}{M})^M \approx \frac{1}{e}$ so that $c_M \leq \frac{OPT}{e}$.

$$\begin{aligned} b_M &= OPT - c_M \\ b_M &= OPT - \frac{OPT}{e} \\ b_M &= OPT\ (1 - \frac{1}{e}) \end{aligned} \tag{31}$$

References

[1] http://thoughtleadership.aonbenfield.com/Documents/20180124-ab-if-annual-companion-volume.pdf
[2] Cisco Visual Networking Index: Forecast and Trends, 2017-2022.
[3] M. Mozaffari, W. Saad, M. Bennis, M. Debbah. "Efficient Deployment of Multiple Unmanned Aerial Vehicles for Optimal Wireless Coverage", IEEE Communications Letters, 20(8):1647-1650, 2016.
[4] L. Ruan, J. Wang, J. Chen, Y. Xu, Y. Yang, H. Jiang, Y. Zhang, Y. Xu. "Energy-Efficient Multi-UAV Coverage Deployment in UAV Networks: A Game-Theoretic Framework", China Communications, 194-209, October 2018.
[5] B. Li, C. Chen, R. Zhang, H. Jiang, X. Guo. "The Energy-efficient UAV-based BS Coverage in Air-to-Ground Communications", IEEE 10th Sensor Array and Multichannel Signal Processing Workshop (SAM), 2018.
[6] M. Alzenad, A. El-Keyi, F. Lagum, and H. Yanikomeroglu. "3D Placement of an Unmanned Aerial Vehicle Base Station (UAV-BS) for Energy-Efficient Maximal Coverage", IEEE Wireless Communications Letters, 6(4), 2017.
[7] M. M. Azari, F. Rosas, K. Chen, and S. Pollin. "Ultra Reliable UAV Communication Using Altitude and Cooperation Diversity", IEEE Transactions on communications, 66(1), pp.330-344, 2018.
[8] H.S. Lee, H.W. Yoo and B.H. Lee. "Deployment Method of UAVs with Energy Constraint for Multiple Tasks", IEEE Electronic Letters, 51(21), 1650–1652, 2015.

[9] S. Kandeepan, K. Gomez, L. Reynaud, T. Rasheed. "Aerial-Terrestrial Communications: Terrestrial Cooperation and Energy-Efficient Transmissions to Aerial Base Stations", IEEE Transactions on Aerospace and Electronic Systems, 50(4), pp.2715-2735, 2014.
[10] A. Merwaday, A. Tuncer, A. Kumbhar, and I. Guvenc. "Improved Throughput Coverage in Natural Disasters Unmanned Aerial Base Stations for Public-Safety Communications", IEEE Vehicular Technology Magazine, pp.53-60, 2016.
[11] M. Mozaffari, W. Saad, M. Bennis, and M. Debbah. "Wireless Communication Using Unmanned Aerial Vehicles (UAVs): Optimal Transport Theory for Hover Time Optimization", IEEE Transactions on Wireless Communications, 16(12), pp.8052-8066, 2017.
[12] Z. Xiao, B. Zhu, Y. Wang, Pu Miao. "Low-Complexity Path Planning Algorithm for Unmanned Aerial Vehicles in Complicated Scenarios", IEEE Access, vol. 6: 57049-57055, 2018.
[13] J. Tao, C. Zhong, L. Gao, H. Deng. "A Study on Path Planning of Unmanned Aerial Vehicle Based on Improved Genetic Algorithm", IEEE 8th International Conference on Intelligent Human-Machine Systems and Cybernetics, 2016.
[14] J. L. Foo, J. Knutzon, V. Kalivarapu, J. Oliver, and E. Winer. "Path Planning of Unmanned Aerial Vehicles Using B-Splines and Particle Swarm Optimization" Journal of Aerospace Computing Information and Communication 6:271-290, 2009.
[15] M. Bekhti, M. Abdennebi, N. Achir, K. Boussetta. "Path Planning of Unmanned Aerial Vehicles With Terrestrial Wireless Network Tracking" Wireless Days 2016,Toulouse, France.
[16] Vijay V. Vazirani "Approximation Algorithms", Springer, 2001.
[17] A. Biniaz, P. Liu, A. Maheshwari, M. Smid. "Approximation Algorithms for the Unit Disk Cover Problem in 2D and 3D. Elsevier Computational Geometry: Theory and Applications", vol.60 pp.8–18, 2017.
[18] X. Gao, J. Fan, F. Wu and G. Chen. "Approximation Algorithms for Sweep Coverage Problem With Multiple Mobile Sensors", IEEE/ACM Transactions on Networking, 26(2), pp.990-1003, 2018.
[19] A. Al-Hourani, S. Kandeepan, and S. Lardner. "Optimal LAP Altitude for Maximum Coverage", IEEE Wireless Communication Letter, 3(6):569-572, 2014.
[20] R. Yaliniz, A. El-Keyi, and H. Yanikomeroglu. "Efficient 3-D placement of an aerial base station in next generation cellular networks", in Proc. of IEEE International Conference on Communications (ICC), Kuala Lumpur, Malaysia, May 2016.
[21] A. Al-Hourani, S. Kandeepan, and A. Jamalipour. "Modeling Air-to-Ground Path Loss for Low Altitude Platforms in Urban Environments," IEEE Global Communications Conference, Austin, TX, USA, 2014.
[22] Code of Federal Regulations, Title 14 Aeronautics and Space, Parts 60 to 109, "Small Unmanned Aircraft Regulations (Part 107)", Revised as of January 1, 2018.
[23] H. Ghazzai, M. B. Ghorbel, A. Kadri, J. Hossain, and H. Menouar. "Energy-Efficient Management of Unmanned Aerial Vehicles for Underlay Cognitive Radio Systems", IEEE Transactions on Green Communications and Networking, 1(4), 434-443, 2017.
[24] J. V. Dries Hulens and T. Goedeme. "How to choose the best embedded processing platform for onboard UAV image processing", International Joint Conference Computer Vision, Imaging and Computer Graphics Theory and Applications (VISIGRAPP), Berlin, Germany, 2015.
[25] https://www2.cs.duke.edu/courses/fall13/compsci530/notes/lec16.pdf
[26] http://ardupilot.org/dev/docs/sitl-native-on-windows.html
[27] D'Hondt, Victor. "La representation proportionelle des parties", 1878.
[28] D'Hondt, Victor. "Systeme pratique et raisonne de representation proportionelle", 1882.
[29] D. Gross, J.F. Shortle, J.M. Thompson, C.M. Harris. "Fundamentals of Queueing Theory", Fourth Edition, A John wiley & Sons, Inc., Publication, 2008.
[30] K. J. Nurmela and P. R. J. Ostergard. "Covering Square with up to 30 Equal Circles", Helsinki University of Technology, Laboratory for Theoretical Computer Science, 2000.

Elif Bozkaya received her MSc degree in Computer Engineering from Istanbul Technical University, Turkey in 2015. Recently, she also received her PhD in 2020 from the same department in Istanbul Technical University. She was visiting researcher in Faculty of Computer Science in University of Vienna, Austria, between February-August 2019. Currently, she is Teaching Staff at the Department of Computer Engineering in National Defense Naval Academy, Turkey. She is the recipient of IEEE INFOCOM Best Paper Award (2018). Her research interest includes Aerial Networks, Software-Defined Networking (SDN), Vehicular Networks, Sensor Networks.

Klaus-Tycho Foerster is a PostDoc at the Faculty of Computer Science at the University of Vienna, Austria since 2018. He received his Diplomas in Mathematics (2007) & Computer Science (2011) from Braunschweig University of Technology, Germany, and his PhD degree (2016) from ETH Zurich, Switzerland, advised by Roger Wattenhofer. He spent autumn 2016 as a Visiting Researcher at Microsoft Research Redmond with Ratul Mahajan, joining Aalborg University, Denmark as a PostDoc with Stefan Schmid in 2017. His research interests revolve around algorithms and complexity in the areas of networking and distributed computing.

Stefan Schmid is a Professor at the Faculty of Computer Science, at University of Vienna, Austria. He obtained his diploma (MSc) in Computer Science at ETH Zurich in Switzerland (minor: micro/macro economics, internship: CERN) and did his PhD in the Distributed Computing Group led by Prof. Roger Wattenhofer, also at ETH Zurich. As a postdoc, he worked at the Technical University of Munich and the University of Paderborn, in Germany. From 2009 to 2015, Stefan Schmid was a senior research scientist at the Telekom Innovation Laboratories (T-Labs) and at TU Berlin in Germany. From 2015 to 2017, Stefan Schmid was a (tenured) Associate Professor at Aalborg University, Denmark, and continued working part-time at TU Berlin, Germany. Since 2015, he serves as the Editor of the Distributed Computing Column of the Bulletin of the European Association of Theoretical Computer Science (BEATCS), since 2016 as Associate Editor of IEEE Transactions on Network and Service Management (TNSM), and since 2019 as Editor of IEEE/ACM Transactions on Networking (ToN). Stefan Schmid received the IEEE Communications Society ITC Early Career Award 2016 and acquired an ERC Consolidator grant in 2019. His research interests revolve around the fundamental and algorithmic problems of networked and distributed systems.

Berk Canberk is an Associate Professor at the Department of Computer Engineering in ITU. Since 2016, he has been also an Adjunct Associate Professor with the Department of Electrical and Computer Engineering at Northeastern University. He serves as an Editor in IEEE Communications Letter, IEEE Transactions in Vehicular Technology, Elsevier Computer Networks and Elsevier Computer Communications. He is the recipient of IEEE Turkey Research Incentive Award (2018), IEEE INFOCOM Best Paper Award (2018), The British Council (UK) Researcher Link Award (2017), IEEE CAMAD Best Paper Award (2016), Royal Academy of Engineering (UK) NEWTON Research Collaboration Award (2015), IEEE INFOCOM Best Poster Paper Award (2015), ITU Successful Faculty Member Award (2015) and Turkish Telecom Collaborative Research Award (2013). His current research areas include Software-Defined Networking (SDN), Intelligent Aerial Networks, and Next Generation Network Management Systems.